Low saturation fluence antiresonant quantum dot SESAMs for MIXSEL integration

Aude-Reine Bellancourt, Yohan Barbarin*, Deran J. H. C. Maas, Mohammad Shafiei, Martin Hoffmann, Matthias Golling, Thomas Südmeyer, and Ursula Keller

Department of Physics, Institute of Quantum Electronics, ETH Zurich, Wolfgang-Pauli-Str. 16, 8093 Zurich, Switzerland.

**Corresponding author: barbarin@phys.ethz.ch*

Abstract: Quantum dot (QD) semiconductor saturable absorber mirrors (SESAMs) offer a larger design freedom than standard quantum well (QW) SESAMs. QD density, QD growth conditions, number of QD-layers, and post-growth annealing were optimized to independently reduce the saturation fluence and adjust the modulation depth for an antiresonant SESAM that supported for the first time passive modelocking of a vertical external-cavity surface emitting laser (VECSEL) with the same spot size on gain and absorber. The same spot size is a requirement for the modelocked integrated external-cavity surface emitting laser (MIXSEL) concept which enables wafer-scale fabrication of the ultrafast semiconductor laser. The antiresonant SESAM design has low dispersion, is less susceptible to growth errors, and is therefore very promising for short pulse generation and MIXSEL integration.

OCIS codes: (140.4050) Mode-locked lasers; (320.7080) Ultrafast devices, (230.4320) Nonlinear optical devices; (160.6000) Semiconductor materials

References and links

1. U. Keller, "Recent developments in compact ultrafast lasers," Nature **424**, 831-838 (2003).
2. M. Kuznetsov, F. Hakimi, R. Sprague, and A. Mooradian, "High-Power (>0.5-W CW) Diode-Pumped Vertical-External-Cavity Surface-Emitting Semiconductor Lasers with Circular TEM00 Beams," IEEE Photon. Technol. Lett. **9**, 1063-1065 (1997).
3. B. Rudin, A. Rutz, M. Hoffmann, D. J. H. C. Maas, A.-R. Bellancourt, E.Gini, T. Südmeyer, and U. Keller, "Highly efficient optically pumped vertical emitting semiconductor laser with more than 20-W average output power in a fundamental transverse mode," Opt. Lett. **33**, 2719-2721 (2008).
4. J. Chilla, S. Butterworth, A. Zeitschel, J. Charles, A. Caprara, M. Reed, and L. Spinelli, "High Power Optically Pumped Semiconductor Lasers," in Photonics West 2004, Solid State Lasers XIII: Technology and Devices, in Proc. SPIE 5332, H. J. H. R. Scheps, ed. (2004), 143-150.
5. U. Keller, K. J. Weingarten, F. X. Kärtner, D. Kopf, B. Braun, I. D. Jung, R. Fluck, C. Hönninger, N. Matuschek, and J. Aus der Au, "Semiconductor saturable absorber mirrors (SESAMs) for femtosecond to nanosecond pulse generation in solid-state lasers," IEEE J. Sel. Top. Quantum Electron. **2**, 435-453 (1996).
6. U. Keller, and A. C. Tropper, "Passively modelocked surface-emitting semiconductor lasers," Phys. Rep. **429**, 67-120 (2006).
7. A. Aschwanden, D. Lorenser, H. J. Unold, R. Paschotta, E. Gini, and U. Keller, "2.1-W picosecond passively mode-locked external-cavity semiconductor laser," Opt. Lett. **30**, 272-274 (2005).
8. K. G. Wilcox, Z. Mihoubi, G. J. Daniell, S. Elsmere, A. Quarterman, I. Farrer, D. A. Ritchie, and A. Tropper, "Ultrafast optical Stark mode-locked semiconductor laser," Opt. Lett. **33**, 2797-2799 (2008).
9. D. Lorenser, D. J. H. C. Maas, H. J. Unold, A.-R. Bellancourt, B. Rudin, E. Gini, D. Ebling, and U. Keller, "50-GHz passively mode-locked surface-emitting semiconductor laser with 100 mW average output power," IEEE J. Quantum Electron. **42**, 838-847 (2006).
10. D. J. H. C. Maas, A.-R. Bellancourt, B. Rudin, M. Golling, H. J. Unold, T. Südmeyer, and U. Keller, "Vertical integration of ultrafast semiconductor lasers," Appl. Phys. B: Lasers Opt. **88**, 493-497 (2007).
11. A.-R. Bellancourt, D. J. H. C. Maas, B. Rudin, M. Golling, T. Südmeyer, and U. Keller, "Modelocked Integrated External-Cavity Surface Emitting Laser (MIXSEL)," IET Optoelectronics **3**, 61-72 (2009).
12. D. A. B. Miller, "Rationale and challenges for optical interconnects to electronic chips," Proc. IEEE **88**, 728-749 (2000).

#108892 - $15.00 USDReceived 18 Mar 2009; revised 14 May 2009; accepted 14 May 2009; published 26 May 2009

13. I. Young, E. Mohammed, J. Liao, Alexandra Kern, S. Palermo, B. Block, M. Reshotko, and P. Chang, "Optical I/O Technology for Tera-Scale Computing," IEEE International Solid-State Circuits Conference 2009 (2009).
14. U. Keller, "Ultrafast solid-state lasers," in Landolt-Börnstein. Laser Physics and Applications. Sub volume B: Laser Systems. Part I. , G. Herziger, H. Weber, and R. Proprawe, eds. (Springer Verlag, Heidelberg, 2007), 33-167.
15. R. Paschotta, R. Häring, U. Keller, A. Garnache, S. Hoogland, and A. C. Tropper, "Soliton-like pulse-shaping mechanism in passively mode-locked surface-emitting semiconductor lasers," Appl. Phys. B: Lasers Opt. **75**, 445-451 (2002).
16. D. J. H. C. Maas, A. R. Bellancourt, M. Hoffmann, B. Rudin, Y. Barbarin, M. Golling, T. Südmeyer, and U. Keller, "Growth parameter optimization for fast quantum dot SESAMs," Opt. Express **16**, 18646-18656 (2008).
17. A. Garnache, S. Hoogland, A. C. Tropper, J. M. Gerard, V. Thierry-Mieg, and J. S. Roberts, "Pico-second passively mode locked surface-emitting laser with self-assembled semiconductor quantum dot absorber," in CLEO/Europe-EQEC, p. postdeadline paper. (2001)
18. E. U. Rafailov, S. J. White, A. A. Lagatsky, A. Miller, W. Sibbett, D. A. Livshits, A. E. Zhukov, and V. M. Ustinov, "Fast quantum-dot saturable absorber for passive mode-locking of solid-state lasers," IEEE Photon. Technol. Lett. **16**, 2439-2441 (2004).
19. C. Scurtescu, Z. Y. Zhang, J. Alcock, R. Fedosejevs, M. Blumin, I. Saveliev, S. Yang, H. Ruda, and Y. Y. Tsui, "Quantum dot saturable absorber for passive mode locking of Nd : YVO4 lasers at 1064 nm," Appl. Phys. B: Lasers Opt. **87**, 671-675 (2007).
20. M. Lumb, D. Farrell, E. Clarke, M. Damzen, and R. Murray, "Post-growth tailoring of quantum-dot saturable absorber mirrors by chemical etching," Appl. Phys. B: Lasers Opt. **94**, 393-398 (2009).
21. R. Grange, M. Haiml, R. Paschotta, G. J. Spuhler, L. Krainer, M. Golling, O. Ostinelli, and U. Keller, "New regime of inverse saturable absorption for self-stabilizing passively mode-locked lasers," Appl. Phys. B:Lasers Opt **80**, 151-158 (2005).
22. T. R. Schibli, E. R. Thoen, F. X. Kärtner, and E. P. Ippen, "Suppression of Q-switched mode locking and break-up into multiple pulses by inverse saturable absorption," Appl. Phys. B: Lasers Opt. **70**, S41-S49 (2000).
23. D.J.H.C Maas, *MIXSEL – a new class of ultrafast semiconductor lasers*, (Hartung-Gorre Verlag, Konstanz, 2009), Chap. 3.
24. D. J. H. C. Maas, B. Rudin, A.-R. Bellancourt, D. Iwaniuk, S. V. Marchese, T. Südmeyer, and U. Keller, "High precision optical characterization of semiconductor saturable absorber mirrors," Opt. Express **16**, 7571-7579 (2008).
25. S. Malik, C. Roberts, R. Murray, and M. Pate, "Tuning self-assembled InAs quantum dots by rapid thermal annealing," Appl. Phys. Lett. **71**, 1987-1989 (1997).

1. Introduction and motivation

Diode-pumped picosecond and femtosecond solid-state lasers have made a large impact since the early 90s in both fundamental science and industrial applications [1]. Nowadays, **v**ertical **e**xternal **c**avity **s**urface **e**mitting **l**asers (VECSELs) [2] start to become a promising alternative to the well established diode-pumped solid-state lasers. VECSELs combine the benefits from diode-pumped solid-state and semiconductor laser technologies with wavelength flexibility, high power and excellent beam quality. Diode-pumped VECSELs produced an average power as high as 22 W with an optical-to-optical efficiency of 43% in a fundamental Gaussian mode [3] and as high as 30 W with a higher order mode of $M^2 \approx 3$ [4]. Modelocking of VECSELs for short pulse generation is typically achieved with an intracavity **se**miconductor **s**aturable **a**bsorber **m**irror (SESAM) [5]. To date, the SESAM-VECSEL modelocking approach [6] resulted in high average power levels (up to 2.1 W average power in 4.7 ps pulses [7]), short pulse durations (260 fs pulses with 25 mW [8]), and high repetition rates (50 GHz with 102 mW in 3.1 ps pulses [9]). Such performance is extremely attractive for many applications, however, the laser contains two separate semiconductor elements in a folded cavity (V-cavity), which is a challenge for cost-efficient high volume fabrication. Recently, we have demonstrated that the SESAM and the VECSEL gain structure can also be integrated into a single semiconductor structure as shown in Fig. 1(b), which is referred to as **m**odelocked **i**ntegrated e**x**ternal-cavity **s**urface **e**mitting **l**aser (MIXSEL) [10, 11]. The compactness and the simplicity of the MIXSEL platform is suitable for mass production and large-scale applications such as optical interconnects between microelectronic chips [12, 13]

#108892 - $15.00 USDReceived 18 Mar 2009; revised 14 May 2009; accepted 14 May 2009; published 26 May 2009

or optical clocking of future high frequency (>10 GHz) multi-core microprocessors. The SESAM integration into a MIXSEL requires specific absorber properties. In contrast to diode-pumped solid-state lasers, a semiconductor gain material exhibits dynamic pulse-to-pulse gain saturation [14, 15]. In order to achieve stable modelocking, the absorber needs to saturate at lower pulse energies than the gain. In standard VECSEL-SESAM modelocking, this is usually achieved by strong focusing onto the SESAM, which even limits the minimum geometrical size and the maximum achievable repetition rate [7]. In a MIXSEL (Fig. 1(b)), the semiconductor structure represents only ≈10 µm, in a ≈3 mm cavity length in the case of 50 GHz repetition rate. Thus the beam diameters on gain and absorber layers are the same. Modelocking with the same spot-size on gain and absorber requires a reduction of the saturation fluence of the saturable absorber. In the first MIXSEL demonstration, the lower saturation of the absorber was achieved with a single-layer quantum dot (QD) saturable absorber and resonant field enhancement [10, 11]. The relative field strength in the absorber section is controlled by the number of pairs in the intermediate distributed Bragg reflector (DBR) (Fig. 2(a)). The disadvantage of the resonant field enhancement is a higher group delay dispersion (GDD) and a significant sensitivity towards growth errors (Fig. 2(b)). This resulted in a relatively long and not transform-limited pulse duration of 32 ps from the first MIXSEL [10, 11]. Fig. 2(b) illustrates the effect of growth error on the GDD as a function of the lasing wavelength. The GDD easily reaches high values limiting the pulse length. QD-saturable absorber layers with lower saturation energy allow for an antiresonant design (Figs. 2(c) and 2(d)), which can strongly improve the growth tolerance and GDD of the MIXSEL.

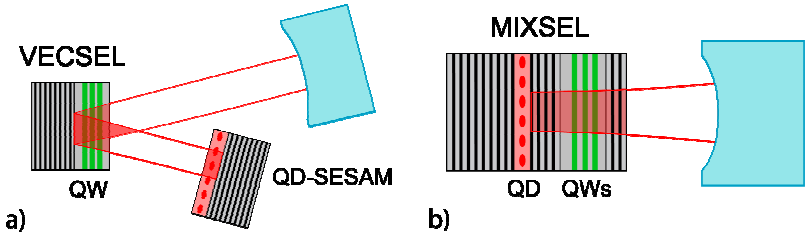

Fig. 1. SESAM-VECSEL modelocking with similar spot areas and MIXSEL concept

In this work, we demonstrate for the first time that an antiresonant SESAM, i.e. a SESAM without field enhancement in the absorber section, can modelock a VECSEL with same spot size on gain and saturable absorber. This demonstration has been made possible thanks to a systematic study on the influence of QD-SESAM growth parameters and post-growth annealing on the macroscopic optical SESAM properties [16]. QD-SESAMs are attractive not only to modelock semiconductor lasers [17, 18], but also solid-state lasers [19, 20], however limited information about their nonlinear response and saturation fluence was available. Here, we experimentally confirm the design guidelines and present an optimized multiple-layer QD-SESAM, which achieves low saturation fluence without any resonant field enhancement and provides sufficient nonlinear modulation depth to modelock the VECSEL. Such absorbers enable MIXSELs with higher growth tolerance and lower dispersion as shown in Figs. 2(c) and 2(d). The optical intensity in the QD-layers is at the same level as in the QWs. One can see in Fig. 2(d) that the tolerance of the antiresonant MIXSEL design against growth errors is much higher than for the resonant design with field enhancement in the absorber region. High tolerance is especially important for the manufacturing requirements of high-volume wafer-scale fabrication [11]. The GDD of the antiresonant MIXSEL design is also reduced and less strongly modulated as a function of wavelength which is beneficial for short pulse generation.

#108892 - $15.00 USDReceived 18 Mar 2009; revised 14 May 2009; accepted 14 May 2009; published 26 May 2009

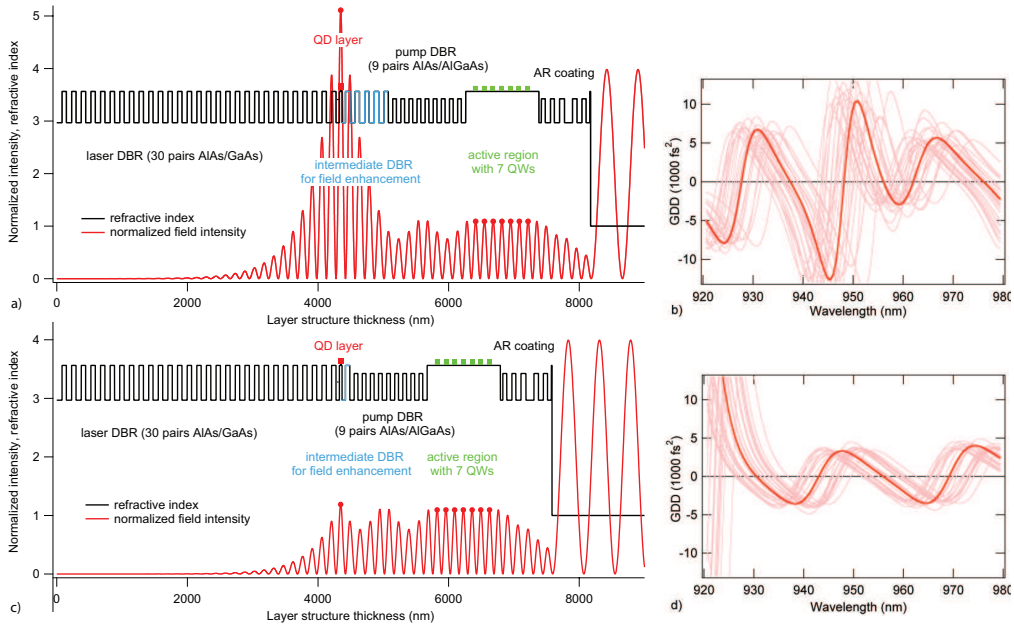

Fig. 2. Refractive index structure (black), calculated standing wave intensity pattern for $\lambda = 960$ nm (red) and the calculated wavelength dependence of the group delay dispersion (GDD) for two different MIXSEL structures using either resonant field enhancement (a and b) or an antiresonant design for the saturable absorber layer (c and d). The different sections are the laser distributed Bragg reflector (DBR), quantum dot (QD) absorber layer, intermediate DBR for field enhancement, pump DBR, active region and antireflective (AR) coating. The graph shows the first resonant MIXSEL design with a 5-pair intermediate DBR for field enhancement (a) and a new antiresonant design (c) with their corresponding GDD (b and d). The GDD is calculated for random material flux variations below 1%, which simulates the growth errors on layer thicknesses occurring in the MBE (thinner traces in b and d).

2. Antiresonant QD-SESAMs with low saturation fluence

The SESAM nonlinear reflectivity is described mainly by the modulation depth ΔR, i.e. the difference in reflectivity between a fully saturated and an unsaturated SESAM, the non-saturable losses Δ_{rns}, and the saturation fluence F_{sat}, which is the pulse fluence (pulse energy per area) for which the SESAM starts to saturate (Fig. 3). The roll-over in Fig. 3 is mostly due to two-photon absorption (TPA) [21, 22] because ≈130 femtosecond pulses have been used. This roll-over is strongly reduced in the picosecond regime [21]. The dashed lines in Fig. 3 indicate the calculated nonlinear reflectivity response without any TPA. QD absorbers have the potential for a fast relaxation [18]. However the relaxation time strongly depends on the growth parameters [16]. The lower density of states with increased confinement and the additional dot density parameter allow for low saturation fluence at moderate modulation depth [10]. In our previous study on the growth parameters and post-growth annealing of single layer QD-SESAM [16], we have demonstrated that the modulation depth can be adjusted with the monolayer (ML) coverage (i.e. QD density) without changing the saturation fluence. This is a real benefit of QD absorbers compared to QW absorbers. In addition, it was possible to substantially reduce the saturation fluence with post-growth annealing when the ML coverage was not too high. Depending on the annealing time and temperature, we could reduce the saturation fluence of QD-SESAMs up to a factor of ten [16]. The annealing reduces the photoluminescence bandwidth and, in most cases, increases the signal amplitude, which indicates an improvement of the dot quality.

#108892 - $15.00 USDReceived 18 Mar 2009; revised 14 May 2009; accepted 14 May 2009; published 26 May 2009

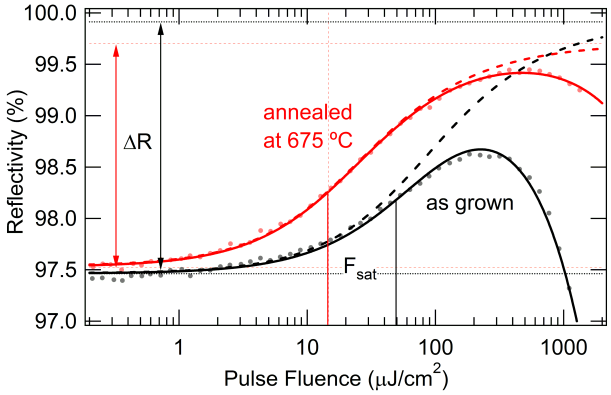

Fig. 3. Measured nonlinear optical reflectivity of an as-grown and annealed QD-SESAM grown at 420°C with 4 QD-layers and ≈ 2 monolayers (ML) InAs coverage. The rollover that appears on both curves is mainly due to two-photon absorption (TPA) [21, 22], because ≈130 fs pulses have been used for the measurement. The dashed line shows the calculated nonlinear reflectivity response without TPA, which more closely represents the picosecond pulse regime [21].

The modulation depth of the low-saturation-fluence, annealed, single-layer and antiresonant QD-SESAMs is ≈0.5 %, which is too low for modelocking our VECSELs without significant soliton pulse shaping [15]. Higher modulation depth results in a larger modelocking stability region, however if the SESAM is not completely saturated the average output power drops because of the larger losses [23]. We therefore increased the number of absorber layers. The design of our multilayer antiresonant QD-SESAM is presented in Fig. 4. The DBR is a 30 pair AlAs/GaAs mirror centered at 960 nm and has a theoretical reflectivity of 99.99 %. The QD section is grown on top of the DBR. The InAs QDs are spaced by 12 nm and are embedded between thin GaAs layers. With only 3 QD-layers we placed them all around the same antinode of the standing wave intensity pattern. With 4 QD-layers as shown in Fig. 4, we placed only two QD-layers in two subsequent antinodes of the standing wave. The design is antiresonant, which means that the electrical field at the surface of the SESAM has a node (i.e. ideal for low damage), and the field enhancement is strongly reduced. This SESAM design is very insensitive towards growth errors and has very low GDD (± 200 fs^2) over more than 40 nm around the central wavelength.

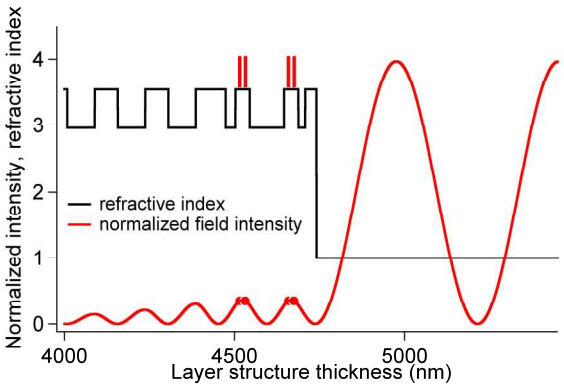

Fig. 4. Refractive index structure (black) and normalized field intensity pattern (red) of a 4-layer antiresonant QD-SESAM design. The structure contains a 30-pair DBR with a saturable absorber section grown on top.

#108892 - $15.00 USDReceived 18 Mar 2009; revised 14 May 2009; accepted 14 May 2009; published 26 May 2009

We used a very accurate measurement set-up [24] to determine the saturation fluence and modulation depth of the different QD-SESAMs. Table 1 summarizes the results for a SESAM with 4 QD-layers grown at 420°C, with ≈2 ML of Indium coverage and annealed at different temperatures (600-675°C). The annealing changes the dot composition (Indium out diffusion) and size, resulting in a blue shift of the absorption and PL emission wavelengths [25]. Similar to our previous measurements on single layer QD-SESAMs, the saturation fluence can be tuned by the annealing temperature [16] whereas the modulation depth does not change significantly. The non-saturable losses increase slightly by ≈0.1 % after the annealing procedure. The final total non-saturable loss is still very low with only ≈10 % of the modulation depth. The post-growth annealing is performed in an RTA for one hour. The samples are protected during the annealing with 200 nm silicon dioxide. The silicon dioxide is removed afterwards in a reactive ion etching (RIE), which might damage the surface of the samples. We therefore would prefer insitu annealing inside the MBE chamber in the future. The samples cannot be annealed at significantly higher temperature than presented here, it would damage the material because of the degassing of Arsenic. This would severely increase the non-saturable losses. Furthermore at higher temperature, the blue shift of the QDs absorption [25] might be too large and the QDs would become transparent at the wavelength of interest.

Table 1. Saturation fluence and modulation depth of the 4-layers QD-SESAMs grown at 420ºC and annealed for 1 hour at different temperatures. For the modulation depth, we assumed no effect from two photon absorption. (Fig. 3 dashed line).

Annealing temperature	*Fitted* F_{sat} (μJ/cm^2)	*Fitted* ΔR (%)	*Non-saturable losses (%)*
as grown	49.7	2.37	0.10
600ºC	40.4	2.05	0.13
625ºC	30.0	2.1	0.21
675ºC	14.7	2.2	0.22

We have compared the saturation fluence and modulation depth of QD-SESAMs with 3 and 4 QD-layers for three different levels of Indium coverage (1.8, 2.0 and 2.12 ML). The results are shown in Fig. 5 for samples kept as grown and annealed at 675°C for one hour. The influence of Indium coverage and annealing is similar to the single-layer QD-SESAMs [16]. The modulation depth increases with the Indium coverage (i.e. dot density) while the saturation fluence remains approximately constant. Our measurements confirm that the modulation depth is proportional to the number of QD-layers. In addition, the annealing reduces the saturation fluence to a significantly lower level independent of the number of QD-layers and without changing the modulation depth (Fig. 5).

#108892 - $15.00 USDReceived 18 Mar 2009; revised 14 May 2009; accepted 14 May 2009; published 26 May 2009

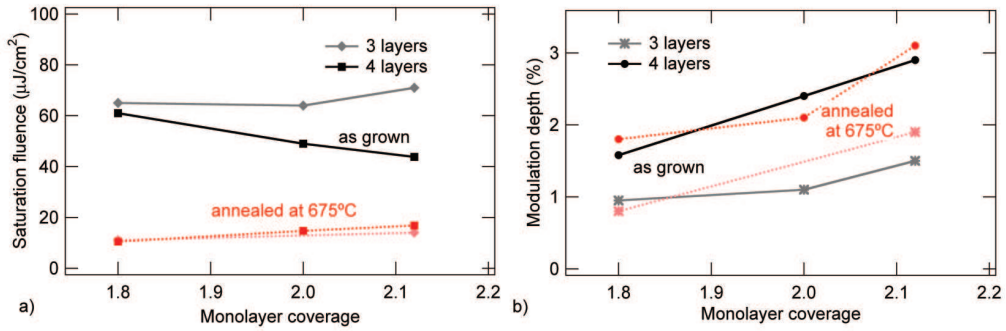

Fig. 5. a) Saturation fluence and b) modulation depth of the 3-layer and 4-layer QD-SESAM grown at 420ºC and annealed for 1 hour at 675°C.

The SESAM recovery dynamics have a direct influence on the pulse duration in a modelocked laser without significant soliton pulse shaping [15]. The growth parameters of the QD-SESAM influence the recovery dynamics and we measured behavior comparable to our previous single layer QD-SESAMs [16].

3. Modelocking results

The antiresonant QD-SESAM with 4 QD-layers and 2.0 ML indium coverage has been tested in a V-shaped laser cavity with same spot areas on the VECSEL gain chip and on the QD-SESAM (Fig. 1(a)). For the first time, modelocking was demonstrated in such a configuration with an antiresonant SESAM. The QD-SESAM annealed at 675ºC for one hour showed the best modelocking performance with the shortest pulses. It has a modulation depth of 2.1 %, a saturation fluence of 14.7 μJ/cm² and 0.22% non-saturable loss. Pulses of 13.5 ps have been obtained at 2.96 GHz and 90 mW average output power (Fig. 6). The pump radius was ≈ 80 μm whereas the laser beam radius on the VECSEL was estimated to ≈ 88 μm, and ≈ 83 μm on the SESAM, which corresponds to a surface ratio of ~1.11. The pulse length is mainly limited by the recovery dynamics of the QD-SESAM and the dispersion of the VECSEL gain chip which is not completely negligible (+1800 fs^2). Achieving modelocking in a 1:1 configuration allows the realization of a MIXSEL with an antiresonant design which has lower dispersion than the initial design and greatly increased growth tolerance as shown in Figs. 2(c) and 2(d).

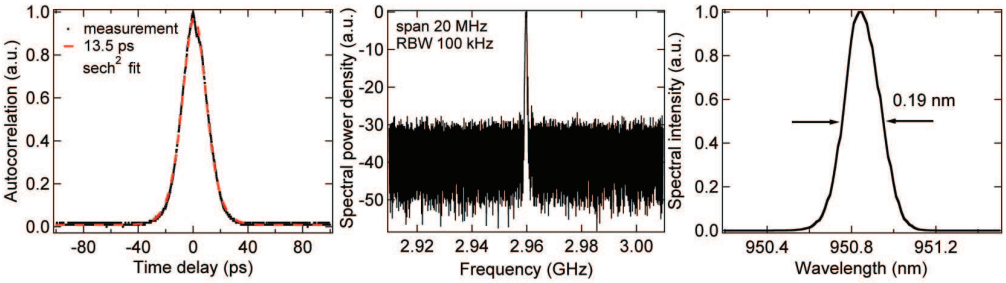

Fig. 6. Pulse characterization of the modelocking result with 90 mW average output power. Left: autocorrelation with sech2-fit using a 13.5 ps pulse duration, middle: pulse repetition rate signal at 2.96 GHz on a microwave spectrum analyzer using a 20 MHz span with 100 kHz resolution bandwidth and right: optical spectrum with a FWHM bandwidth of 0.19 nm measured with an optical spectrum analyzer and a resolution bandwidth of 0.1 nm. The time-bandwidth product is 0.87.

#108892 - $15.00 USDReceived 18 Mar 2009; revised 14 May 2009; accepted 14 May 2009; published 26 May 2009

4. Conclusions

In summary, we have demonstrated the first antiresonant low saturation fluence QD-SESAM for VECSEL modelocking, by studying the effect of growth parameters and post-growth annealing on the macroscopic optical properties of QD-SESAMs. We can independently adjust the saturation fluence and modulation depth because the modulation depth is directly proportional to the ML coverage (i.e. QD density) and the number of QD-layers, while the saturation fluence remains approximately constant. Post-growth annealing improves the QD quality and significantly reduces the saturation fluence. For the first time, we have achieved modelocking with the same mode areas on the VECSEL and the SESAM with such an antiresonant design. The antiresonant design with its reduced GDD is very promising for achieving passively modelocked VECSELs with higher pulse repetition rates and shorter pulse durations. Furthermore, the antiresonant QD saturable absorber substantially simplifies the MIXSEL design and provides better growth tolerance and lower GDD.

Acknowledgements

This work was supported in part by the Intel Corporation through a university sponsored research agreement, the European Network of Excellence ePIXnet and ETH Zurich with the FIRST clean-room facility.

#108892 - $15.00 USDReceived 18 Mar 2009; revised 14 May 2009; accepted 14 May 2009; published 26 May 2009